Hindawi Publishing Corporation
Science and Technology of Nuclear Installations
Volume 2016, Article ID 9542121, 8 pages
http://dx.doi.org/10.1155/2016/9542121

Research Article

Assessment of Prediction Capabilities of COCOSYS and CFX Code for Simplified Containment

Jia Zhu,[1] Xiaohui Zhang,[1] and Xu Cheng[2]

[1]*School of Energy, Soochow University, Suzhou 215000, China*
[2]*Karlsruhe Institute of Technology (KIT), 76131 Karlsruhe, Germany*

Correspondence should be addressed to Xiaohui Zhang; xhzhang@suda.edu.cn

Received 4 February 2016; Accepted 8 May 2016

Academic Editor: Keith E. Holbert

The acceptable accuracy for simulation of severe accident scenarios in containments of nuclear power plants is required to investigate the consequences of severe accidents and effectiveness of potential counter measures. For this purpose, the actual capability of CFX tool and COCOSYS code is assessed in prototypical geometries for simplified physical process-plume (due to a heat source) under adiabatic and convection boundary condition, respectively. Results of the comparison under adiabatic boundary condition show that good agreement is obtained among the analytical solution, COCOSYS prediction, and CFX prediction for zone temperature. The general trend of the temperature distribution along the vertical direction predicted by COCOSYS agrees with the CFX prediction except in dome, and this phenomenon is predicted well by CFX and failed to be reproduced by COCOSYS. Both COCOSYS and CFX indicate that there is no temperature stratification inside dome. CFX prediction shows that temperature stratification area occurs beneath the dome and away from the heat source. Temperature stratification area under adiabatic boundary condition is bigger than that under convection boundary condition. The results indicate that the average temperature inside containment predicted with COCOSYS model is overestimated under adiabatic boundary condition, while it is underestimated under convection boundary condition compared to CFX prediction.

1. Introduction

The containment phenomenological aspects during an accident have been studied extensively during the last 40 years for light water reactors [1–4]. Nevertheless, the Fukushima accident has driven the attention of the regulatory bodies and the industry to the assessment of the detailed thermal-hydraulic containment simulation under severe accident conditions [5].

Considerable international efforts were dedicated to better understand related phenomena by performing experiments and analytical assessments of their results. Since it is not possible to perform containment thermal-hydraulics experiments in the existing nuclear power plants due to safety concerns, experiments are performed in special facilities, which imitate containment or their parts [6, 7]. However, such devices are usually smaller in size and have simpler geometry than prototypical containment. Therefore, in order to study processes on the containment scale, numerical experiments are also performed using computer codes. Codes are also used for simulation of experiments, in order to better understand experimental results, and to assess code capability to simulate occurring processes.

Two main kinds of codes/approaches are used for simulation of containment thermal-hydraulics, that is, lumped-parameter approach with highly simplified 0D models and 3D CFD (Computational Fluid Dynamics) approach.

The program COCOSYS, a lumped-parameter code, is being developed by the Gesellschaft für Anlagen-und Reaktorsicherheit (GRS) gGmbH, Germany, for the simulation of all relevant processes and plant states during severe accidents in containment of light water reactors. And this code is widely used in nuclear engineering [8, 9]. The characteristic feature of lumped-parameter approach is that mass and energy are transferred between control volumes by junctions, according to momentum equation solution for each junction.

The CFX code is a general purpose CFD tool developed by ANSYS Inc. The code solves the conservation equations for mass, momentum, and energy together with their initial

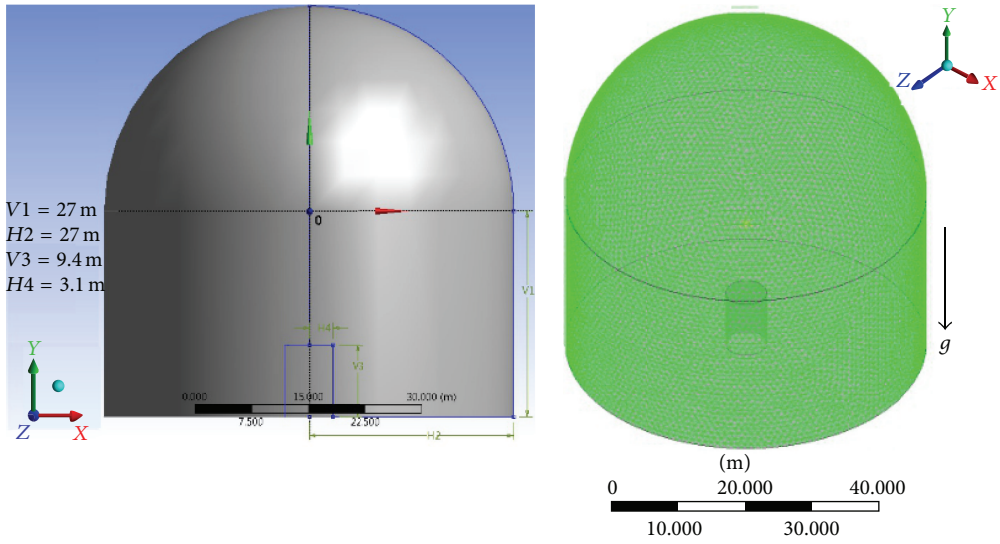

Figure 1: Geometry (a) and mesh (b) for CFD simulation.

and boundary conditions. The discretization of the equations in the CFX code is based on a conservative finite-volume method.

Considerable research has been devoted to the study of the associated phenomena predicted by lumped-parameter code and field code; the development of various computer codes to analyze these severe accidents phenomena is summarized in the review [10].

Nevertheless containment thermal-hydraulics prediction remains an open question. One outcome of the ISP-47 (TOSQAN, MISTRA, and THAI) [11] activity was the recommendation to elaborate generic containment including all important components. In the frame of the European Network of Excellence SARNET2 (Severe Accident Research Network) such generic containment nodalisation was developed, based on an existing COCOSYS model of a German pressurized water reactor (PWR) with 1300 MWe, provided by GRS [12]. It is used to compare and to assess analyses being performed with different lumped-parameter (LP) codes and models. Moreover, it can serve as a basis for testing new model developments on a commonly available and accepted basis on plant scale in future.

In present work, a simplified enclosure based on generic containment is adapted in prototypical geometries for comparing different simulation results with separate effects scenario "thermal plume" to illustrate the prediction capacity of COCOSYS and ANSYS CFX.

2. Assessment of COCOSYS and CFX Prediction Results

Irrespective of the nature of the accident, heat and mass transfer play a major role in these accidents. Quite often it is a complex phenomenon involving forced and natural convection heat transfer, metal-water reaction, nuclear heat generation, melting, condensation, diffusive and convective mass transfer, nucleate and film boiling, porous medium, combustion, and detonation.

The analyses presented here aimed at investigating the accuracy of COCOSYS code compared to the CFD codes to provide an evaluation of the applicability to the large-scale, transient problems. To this aim, the assessment must use separate-effect simulation, so we focus on a plume (due to a heat source) process in the present work; on the other hand, because of the thin shell and cylinder structure in CFX model, measures of smaller structure thickness with higher structure conductivity, lower density, and heat capacity are taken in COCOSYS model to eliminate the transient process impact of the structure, so that COCOSYS model and CFX model are comparable.

2.1. Computational Modeling. Figure 1 shows the geometry of the CFD simulation physical modeling. The main characteristics of the simplified containment are the following: a volume of about 102724 m^3, including a cylinder with radius of 27 m and a height of 27 m, and a hemisphere with radius of 27 m. R-CAVITY (radius $H4 = 3.1$ m; height $V3 = 9.4$ m) is the system heat source with constant value 3000 kW; the rest of space is full of air. The turbulence k-ε model and nonsteady method were used in the calculations.

After grid independent test (coarse, intermediate, and fine mesh), mesh containing tetra element (element size 1.0 m) is adopted; it is simulated in CFX with a 3D Cartesian geometry model using 90,142 computational elements with 1234,062 nodes. Figure 1 shows a 3D view of the domain mesh.

The input data and nodalisation of the generic containment have been created on the basis of benchmark run-2 COCOSYS code for German PWR simulation [12]. Figure 2 shows the COCOSYS model; finer vertical nodalisation is built with 46 zones.

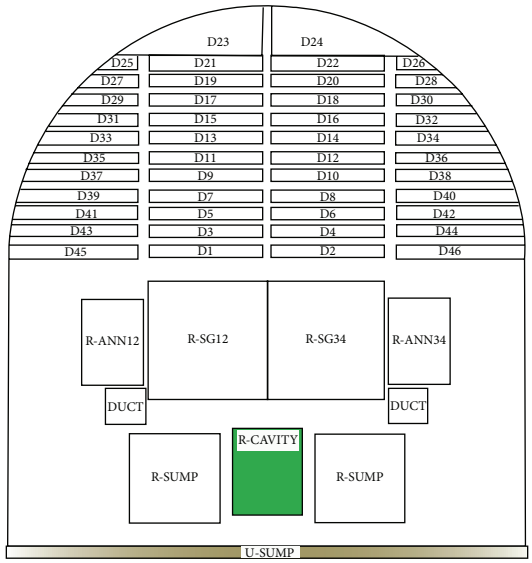

Figure 2: COCOSYS model.

An overview of the general initial condition and boundary condition is listed as follows.

(1) Adiabatic case:

Initial condition: air at 1 bar pressure and 20°C temperature.

R-CAVITY volumetric heat generation: 3000 kW.

Boundary condition: adiabatic enclosure.

(2) Convection case:

Initial condition: air at 1 bar pressure and 20°C temperature.

R-CAVITY volumetric heat generation: 3000 kW.

USUMP boundary condition: adiabatic condition.

More specific information on the convection condition which follows in Section 2.3.

2.2. Adiabatic Case. Direct comparison of the zone temperature in COCOSYS and discrete point temperature is difficult due to some differences between COCOSYS and CFX; an alternative approach is to take a weighted average of CFX discrete points corresponding to COCOSYS area temperature.

The results are compared in curve charts for transient evolution process in Figure 3 at R-SG12 zone.

The x-axis in the graph is the time, y-axis represents temperature, the blue line is the analytical solution of average temperature inside the containment, the dotted black line is transient temperature in R-SG12 zone predicted by COCOSYS, and the dotted red line is CFX predicted average temperature of R-SG12 zone. A relative good agreement is obtained among the analytical solutions, COCOSYS

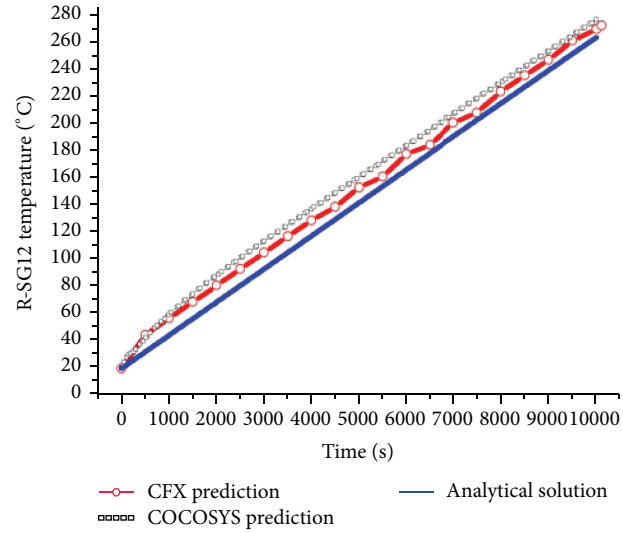

Figure 3: Comparison of zone temperature at transient state.

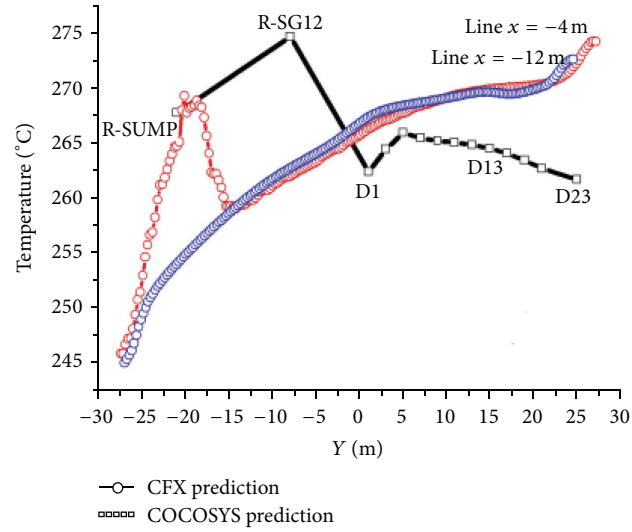

Figure 4: Comparison of temperature distribution at 10106 s.

predicted results, and the CFX predicted results. Figure 4 gives the comparisons of the temperature distribution along the vertical direction inside the containment at 10,106 s. There are 14 layers (R-SUMP, R-SG12, D1, D3, D5, D7, D9, D11, D13, D15, D17, D19, D21, and D23) in COCOSYS model (Figure 2), so 14 points are used for plotting the COCOSYS predicted data (black line in Figure 4).

Two vertical lines ($x = -4$ m and $x = -12$ m in Figure 1) are taken in CFX model to represent the 14 layers' zones in COCOSYS model. It can be seen that near the heat source zone (R-SG12 in COCOSYS, $x = -4$ m in CFX), the temperatures climb up dramatically along the vertical height. It indicates that the general trends of the results for COCOSYS meet an agreement with the CFX prediction (line $x = -4$ m) except in the upper dome.

CFX predictions (line $x = -4$ m and line $x = -12$ m) show that the temperature increases slowly from the height of 3 m

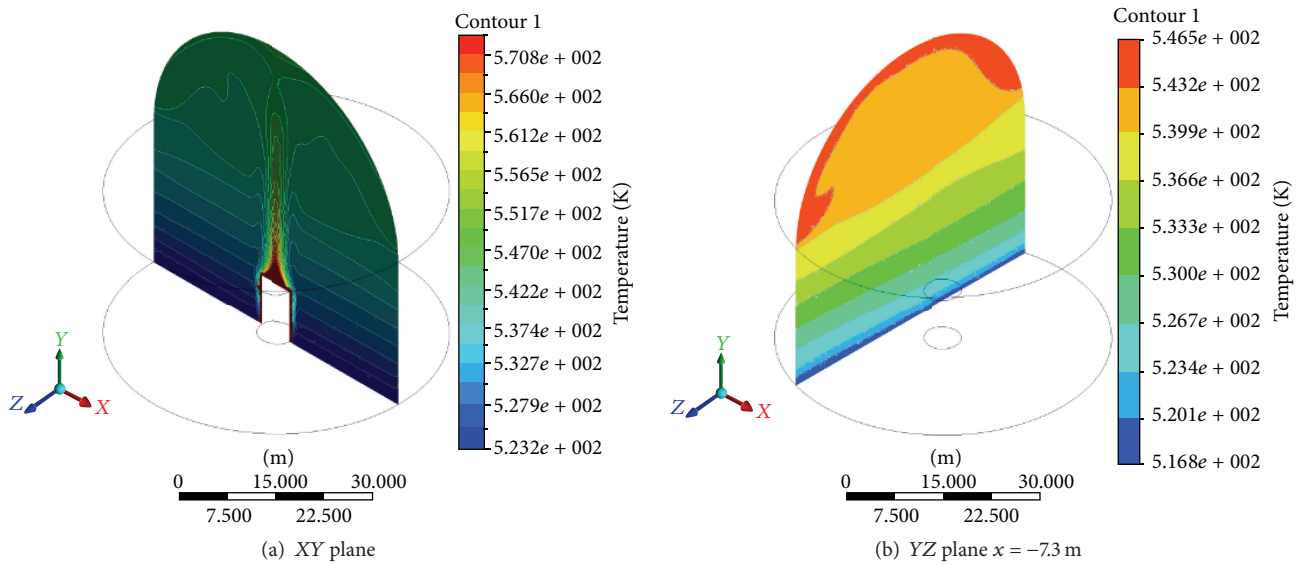

(a) *XY* plane (b) *YZ* plane $x = -7.3$ m

Figure 5: Contour plot of the temperature at 10106 s.

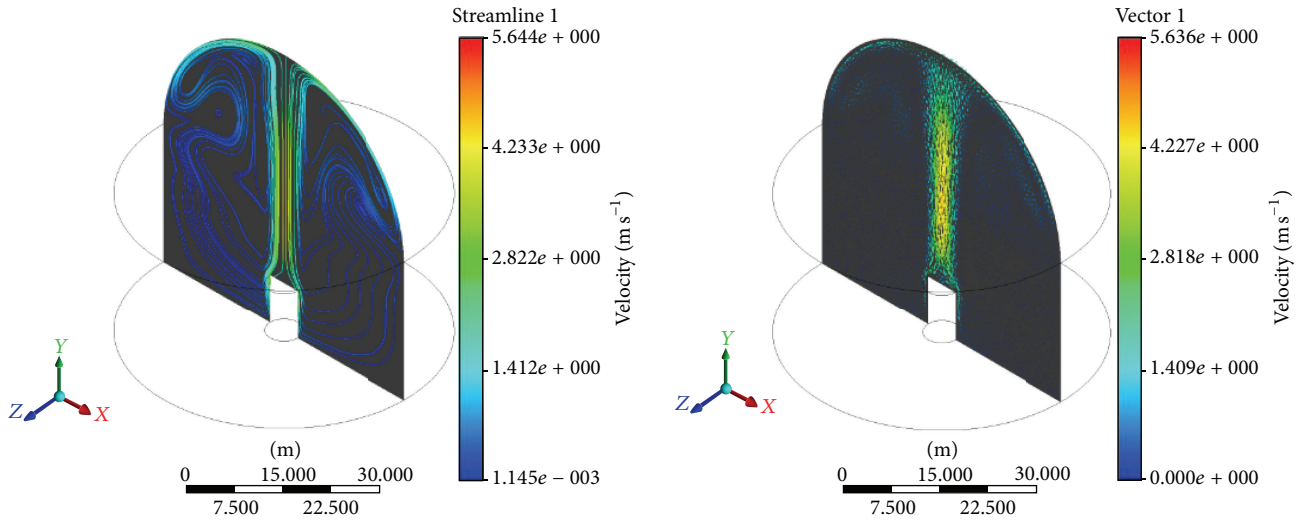

(a) *XY* plane stream line (b) *XY* plane velocity vector

Figure 6: Stream lines and velocity vector at 10106 s.

to 25 m and maintains a relatively high temperature, which implies that most energy is stored in the upper region. In the upper part of the containment the temperature increases again due to the shape of the dome in which the heat can be accumulated; these considerations are seen more clearly in terms of temperature contour map (Figure 5). However, from a quantitative view point, discrepancies are observed in the upper dome between CFX and COCOSYS results. The COCOSYS code gives lower temperature values. CFX prediction (line $x = -12$ m) shows that thermal stratification is more pronounced from the height of $y = -23$ m to $y = 0$ m, which can be seen in temperature contour map (Figure 5); COCOSYS cannot predict thermal stratification, because R-SG12 is big control volume using the equilibrium zone model; from the thermodynamic point of view, the volume temperature is assumed to be mixed homogeneously as zone temperature; the detailed information cannot be obtained from COCOSYS model. The buoyancy-driven flow that arises from the temperature field is presented in Figure 6. It implies that the strong convection areas are in the top of heat source; the weak convection dominant areas are away from the heat source, which suggests an influence of temperature stratification.

It can be seen that the model and boundary conditions are selected symmetric along y-axis, while the contour plot of the temperature (presented in Figure 5) is not very symmetric; the reason is that the symmetric solution breaks down as instabilities grow and the time behaviors of quantities relative to geometrically symmetric points begin to differ; we only presented results at 10,106 s here.

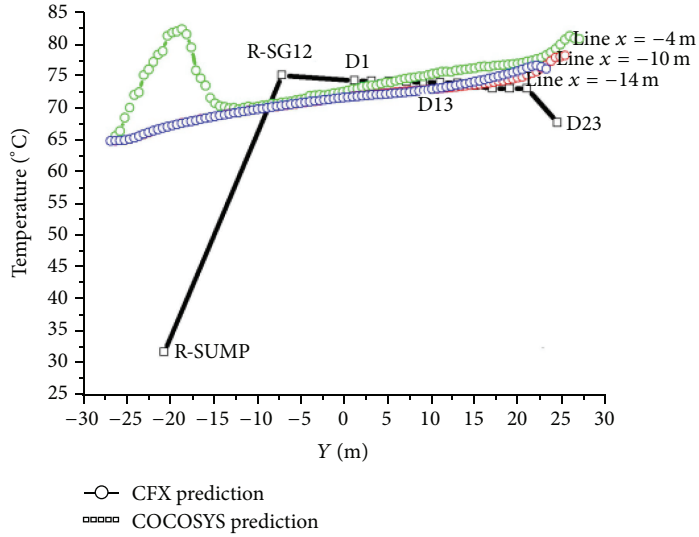

Figure 7: Comparison of temperature distribution.

2.3. Convective Case. For the sake of ensuring the comparability between CFD and COCOSYS, the following should be mentioned here:

(1) The size of the system under consideration makes the computations very time-consuming. The running time (or CPU time) is in the range of 2 months per run to reach thermal equilibrium with CFD if the convective heat transfer coefficient is about 10 W/(m^2 · °C); this large computational overhead strongly limited the scope of analyses. So, here, both COCOSYS and CFD have the same outside convective heat transfer coefficient 100 W/(m^2 · °C). Steady state results are compared for COCOSYS CFX model.

(2) In order to eliminate the wall dynamic inertia delay, measures of higher structure conductivity, lower density, and heat capacity are taken in COCOSYS. Thin shell and plate model with ignoring wall thickness are used in CFD to separate containment enclosure and environment, while it affects the dynamic process, but the steady state will not be affected principally.

There are 14 layers (R-SUMP, R-SG12, D1, D3, D5, D7, D9, D11, D13, D15, D17, D19, D21, and D23) in COCOSYS model, so 14 points are used for plotting the COCOSYS predicted data (Figure 2).

Three vertical lines ($x = -4$ m, $x = -10$ m, and $x = -14$ m in Figure 1) are taken in CFX model to represent the 14 layers zones in COCOSYS model (Figure 2).

Comparisons of right part zones between COCOSYS prediction and CFX prediction are shown in Figure 7.

It can be readily seen that near the heat source zone (R-SG12 in COCOSYS, $x = -4$ m in CFX), the temperatures increase rapidly along the vertical height. The COCOSYS predicted results from zone D1 to zone D21 are similar to the results from CFX; D23 temperature decreasing shown in Figure 7 near the wall can be predicted by COCOSYS. But the increasing feature of temperature in the dome predicted by CFX cannot be predicted by COCOSYS.

CFX predictions (line $x = -4$ m, line $x = -10$ m, and line $x = -14$ m) show that the temperature increases slowly from the height of 3 m to 25 m and maintains a relatively high temperature, which implies that most energy is stored in the upper region. In the upper part of the containment the temperature increases again due to the shape of the dome in which the heat can be accumulated. It is apparent to observe from temperature contour map in Figure 8 that the temperature decreases near the wall of the dome, these considerations are seen more clearly in terms of plane contour map, and the reason is that the outside wall is convection boundary condition.

CFX predictions (line $x = -10$ m and line $x = -14$ m) show that thermal stratification is more pronounced from $y = -23$ m to $y = 0$ m, which can be seen in temperature contour map (Figure 8); COCOSYS cannot predict thermal stratification, because R-SG12 is big control volume using the equilibrium zone model; the volume temperature is assumed to be mixed homogeneously as zone temperature from the thermodynamic point of view; the detailed information cannot be obtained from COCOSYS model.

This feature can be verified from the comparison of horizontal temperature distribution for the zones of R-ANN12, SG12, SG34, and R-ANN34 (Figure 9(a)) and the zones of D45, D1, D2, and D46 (Figure 9(b)), the dotted red line is the CFX prediction result, and the black line is the COCOSYS prediction result; the maximum temperature distribution is very well predicted by the CFX, which would be complicated to simulate using COCOSYS; the use of the COCOSYS led to somewhat less accurate results.

On the other hand, the horizontal line along X direction shows that there is no change of the temperature except in region near the thermal plume and boundary wall region.

From Figure 10, it can be seen that the buoyant convection flow is strong on the upper surface of heat source, indicating

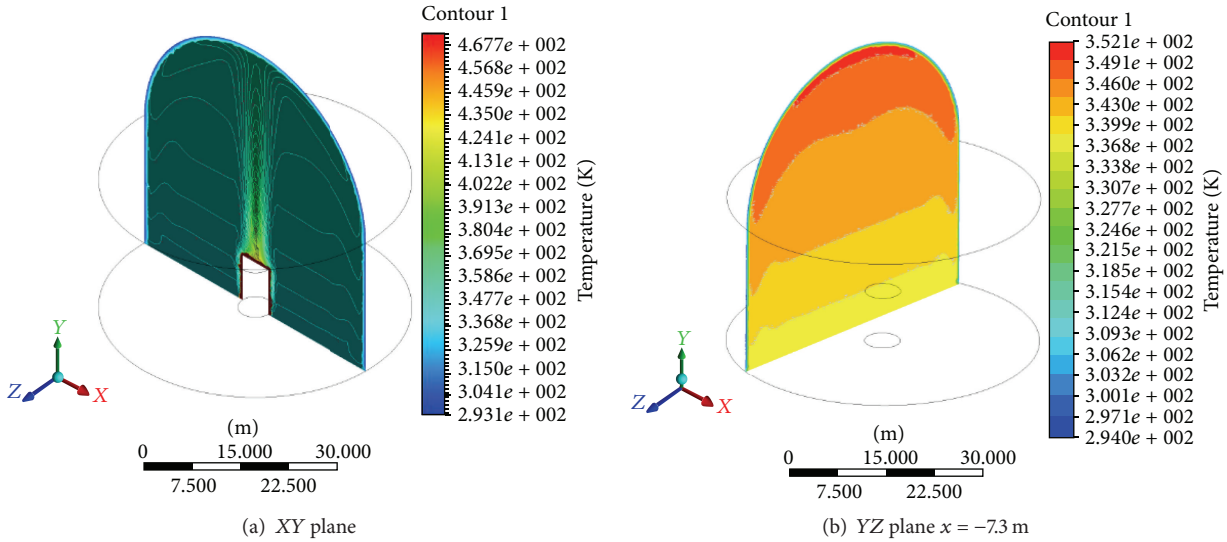

Figure 8: Contour plot of the temperature.

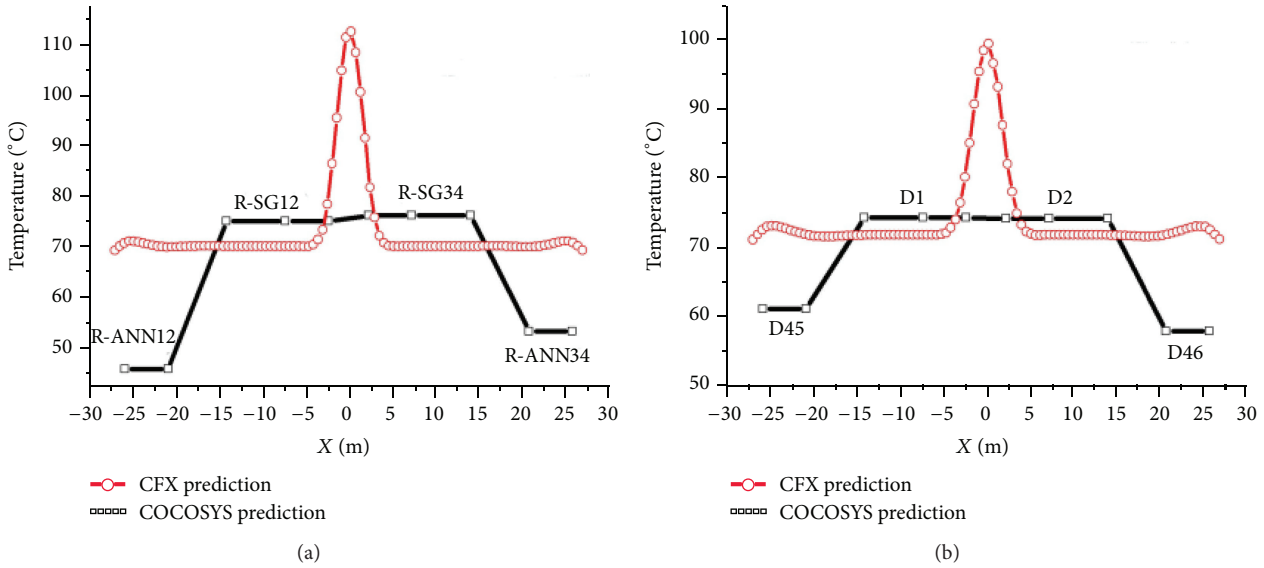

Figure 9: Horizontal temperature distribution.

the strong effect of the natural convection; the weak convection dominant areas are in the two sides of heat source, which suggests an influence of temperature stratification.

For comparison purpose of two boundary conditions, the flow configurations and temperature profiles are different; from Figure 11, it is worth noting that thermal stratification area under convection boundary is smaller than that under the adiabatic boundary. When strongly stratified, enclosure's ambient temperature can be considered one-dimensional, with negligible horizontal gradients except in narrow regions beside the boundary and heat source; on the other hand, there is no thermal stratification area inside the dome area.

3. Conclusion

Main conclusions for separate-effect plume (due to a heat source) simulation between COCOSYS and CFX can be summarized as follows.

Temperature in the upper part of the enclosure is higher for both adiabatic and convection boundary condition; this can be predicted by both COCOSYS and CFX.

Convection intensity affects concentration and temperature stratification; both COCOSYS and CFX can predict that there is no temperature stratification in the upper region of enclosure. Temperature stratification exists in the lower

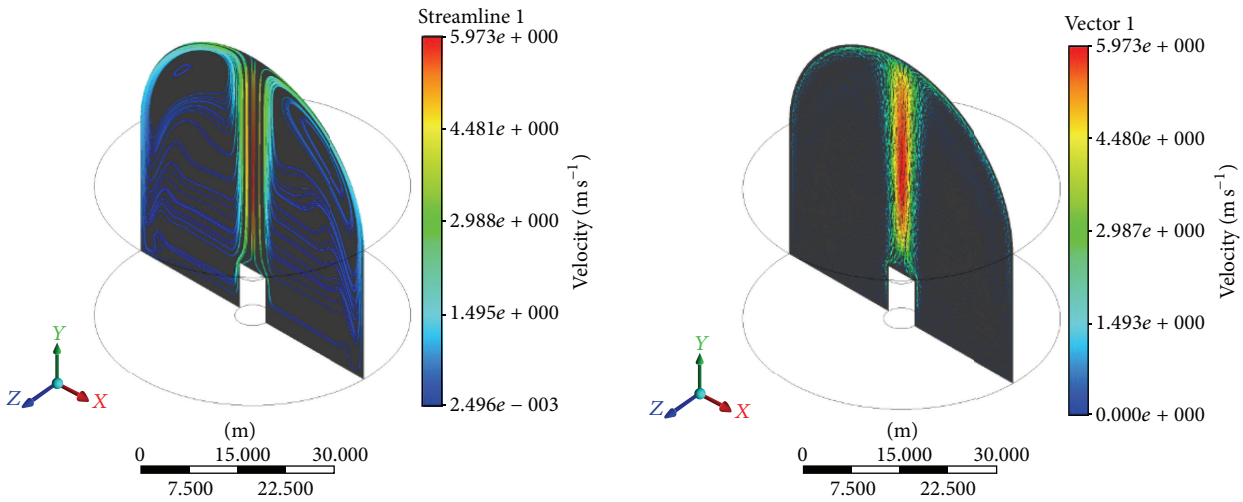

(a) *XY* plane stream line (b) *XY* plane velocity vector

Figure 10: Stream lines and velocity vector.

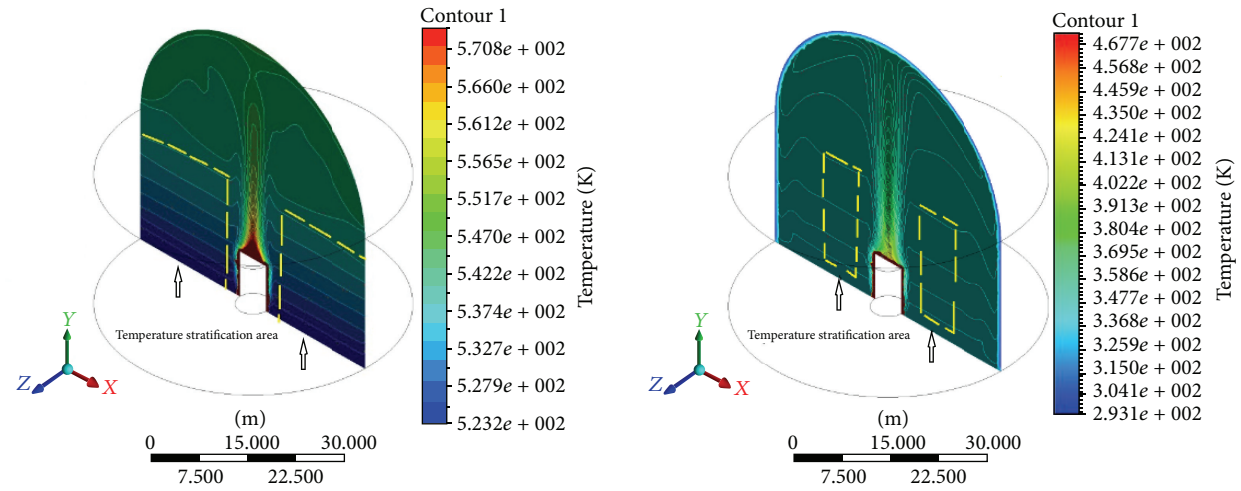

(a) Adiabatic boundary condition (b) Convection boundary condition

Figure 11: Comparison of thermal stratification area.

region of enclosure except in the region near the thermal plume.

Boundary condition affects the temperature stratification. Temperature stratification area under adiabatic boundary condition is bigger than the area under convection boundary condition; CFX are able to predict this phenomenon; however, COCOSYS are not able to predict this phenomenon.

CFX can predict local temperature of thermal plume, while COCOSYS cannot predict local temperature of thermal plume at present nodalisation.

Boundary condition affects the predicted average temperature. The average temperature in enclosure predicted by COCOSYS is overestimated compared to that predicted by CFX under the same adiabatic boundary condition; the average temperature in enclosure predicted by COCOSYS is underestimated compared to that predicted by CFX under the convection boundary condition.

Competing Interests

The authors declare that they have no competing interests.

Acknowledgments

This work is supported by the National Science Foundations of China (51176132). The corresponding author gratefully acknowledges the support of K. C. Wong Education Foundation and DAAD. The corresponding author is approved to use COCOSYS code in KIT Germany.

References

[1] W. Breitung and P. Royl, "Procedure and tools for deterministic analysis and control of hydrogen behavior in severe accidents," *Nuclear Engineering and Design*, vol. 202, no. 2-3, pp. 249–268, 2000.

[2] B. R. Sehgal, "Stabilization and termination of severe accidents in LWRs," *Nuclear Engineering and Design*, vol. 236, no. 19–21, pp. 1941–1952, 2006.

[3] J. Xiao and J. R. Travis, "How critical is turbulence modeling in gas distribution simulations of large-scale complex nuclear reactor containment?" *Annals of Nuclear Energy*, vol. 56, pp. 227–242, 2013.

[4] N. Agrawal, A. Prabhakar, and S. K. Das, "Hydrogen distribution in nuclear reactor containment during accidents and associated heat and mass transfer issues—a review," *Heat Transfer Engineering*, vol. 36, no. 10, pp. 859–879, 2014.

[5] S. Mizokami, D. Yamada, T. Honda, D. Yamauchi, and Y. Yamanaka, "Unsolved issues related to thermal-hydraulics in the suppression chamber during Fukushima Daiichi accident progressions," *Journal of Nuclear Science and Technology*, vol. 53, no. 5, pp. 630–638, 2016.

[6] D. Paladino, M. Andreani, R. Zboray, and J. Dreier, "Toward a CFD-grade database addressing LWR containment phenomena," *Nuclear Engineering and Design*, vol. 253, pp. 331–342, 2012.

[7] A. Dutta, I. Thangamani, V. Shanware et al., "Experiments and analytical studies related to blowdown and containment thermal hydraulics on CSF," *Nuclear Engineering and Design*, vol. 294, no. 1, pp. 233–241, 2015.

[8] M. Povilaitis, T. Kačegavičius, and E. Urbonavičius, "Simulation of the ICE P1 test for a validation of COCOSYS and ASTEC codes," *Fusion Engineering and Design*, vol. 94, no. 1, pp. 42–47, 2015.

[9] I. Kljenak, M. Kuznetsov, P. Kostka et al., "Simulation of hydrogen deflagration experiment—benchmark exercise with lumped-parameter codes," *Nuclear Engineering and Design*, vol. 283, pp. 51–59, 2015.

[10] M. Hashim, Y. Ming, and A. S. Ahmed, "Review of severe accident phenomena in LWR and related severe accident analysis codes," *Research Journal of Applied Sciences, Engineering and Technology*, vol. 5, no. 12, pp. 3320–3335, 2013.

[11] D. C. Visser, N. B. Siccama, S. T. Jayaraju, and E. M. J. Komen, "Application of a CFD based containment model to different large-scale hydrogen distribution experiments," *Nuclear Engineering and Design*, vol. 278, pp. 491–502, 2014.

[12] St. Kelm, M. Klauck, S. Beck et al., "Generic containment: detailed comparison of containment simulations performed on plant scale," *Annals of Nuclear Energy*, vol. 74, pp. 165–172, 2014.